Study on the influence of cavitation development on the performance of nuclear main pump

Study on the influence of cavitation development on the performance of nuclear main pump

X R Cheng[1,2], S Y Zhang[1]

[1] College of Energy and Power Engineering, Lanzhou University of Technology, Lanzhou 730050, China
[2] Key Laboratory of Fluid machinery and Systems, Gansu Province, Lanzhou 730050, China

E-mail: cxr168861@sina.com

Abstract. In order to study the influence of cavitation on the external characteristics and inner flow field of nuclear main pump, based on the continuity equation, Reynolds N-S equation and RNG k-ε turbulence model, the whole flow field cavitation numerical simulation on nuclear main pump model under the design condition is carried out. The performance and internal flow field variation law of the nuclear main pump are obtained through the comparison and analysis when 4 kinds of cavitation conditions are chosen. The results show that the head, efficiency and power of the nuclear main pump have different sensitivities to the reduction of net positive suction head available (NPSHa). With the development of the cavitation process in the pump, the head declines most sharply and the power most moderately. Under the condition of cavitation, the bubbles generated by cavitation have a squeezing effect on the impeller passage, which makes the flow area decrease and the relative velocity of the fluid increase. Meanwhile, the value of maximum velocity appears near the outlet of the blade. Meanwhile, the bubbles generated by cavitation change the flow state of the cavitation region, which makes the kinetic viscosity of fluids, the turbulent dissipation rate and the loss of turbulent dissipation reduce.

1. Introduction

Cavitation exists in many areas, such as fluid machinery, marine engineering, underwater weapons, hydrofoils and culverts. The occurrence of cavitation changes the velocity distribution in the flow path, causing the material denudation and efficiency decrease. With regard to fluid machinery, it makes the turbine power and the pump head lower and leads to machine vibration and noise, affecting the safety and stability of the system operation seriously. Therefore, how to avoid cavitation effectively has become an important aspect in the design of fluid mechanics research [1-3].

The nuclear main pump, " the heart of a nuclear island ", is the only component of a nuclear power plant equipment requiring high-speed operation. Since the nuclear main pump is subject to high temperatures, high pressures and high levels of radiation fluid, its performance and stability is critical to the safety of the entire nuclear power plant [4]. However, cavitation may occur in the nuclear main pump when the primary coolant system breaks down or the loss of heat sink occurs in a nuclear power plant. Therefore, for the safe operation of the nuclear main pump, it is crucial to study the internal flow under the condition of cavitation .

In recent years, many scholars have achieved plenty of researches on the effect of cavitation on the pump. Lu et al [5] investigated the pump inlet and outlet pressure fluctuations, the internal flow instabilities and the vibration characteristics under the condition of unsteady cavitation in a centrifugal pump through numerical simulation and experimental method. It was found that the unsteady cavitation generates as the NPSHa is lower than 5.93m. Chai et al [6] carried out an orthogonal experiment on impeller geometric parameters which exerts an influence on its cavitation performance, designed various impeller hydraulic models with the help of PCAD software and used CFX software to conduct numerical stimulation calculation about its cavitation and hydraulic performance in order to figure out the priority order of factors affecting centrifugal pump cavitation performance. Zhou et al [7] numerically investigated different types of staggering to understand the effects of staggered blades on a canned nuclear coolant pump. The results show that the staggered blade has a vital influence on the performance of canned nuclear coolant pumps. A staggered blade does not boost hydraulic performance but does enhance the axial force and pressure pulsation. Li et al. presented and compared the characteristics of unsteady pressure on the blade surfaces and the symmetric plane of the volute by analyzing internal flows of both with and without cavitations by CFX software. The results showed that the amplitudes of pressure fluctuations of critical cavitation on the blade pressure surface are bigger as compared with those at the non-cavitation condition, whereas on the suction surface, the situation is on the contrary [8]. Guo et al [9] designed 5 inducers with different short blade locations so as to evaluate the effects of the short blade locations on the anti-cavitation performance of the splitter-bladed inducer and the pump. In the meantime, he adopted the algebraic slip mixture model in the CFX software for cavitation simulation. The analysis showed that the short blade locations had a significant effect on the anti-cavitation performance.

The influence of cavitation development on the internal flow field of nuclear main pump is studied in this paper. The whole flow field cavitation simulation of nuclear main pump is carried out by ANSYS CFX software and the influence of cavitation development on the internal flow field of nuclear main pump is obtained.

2. Model description and numerical calculation

2.1. Model parameters

In this study, an AP1400 nuclear main model pump is selected as the research object. The model pump ratio coefficient is λ=0.4. The model pump design parameters are as follows:

Table 1. The main technical parameters of model pump

Design Parameters	Numerical Value
Design Capacity Q_V/(m^3/h)	1385
Design Head H/m	17.8
Rotating Speed n/rpm	1485
Blade Number of Impeller Z_1	5
Blade Number of Guide Vane Z_2	18

2.2. Model description and mesh generation

Figure 1 shows a sketch of the flow-through components of the model pump. The model pump is composed of five main flow parts, namely: the suction section, impeller, guide vane, annular casing, and outlet section.

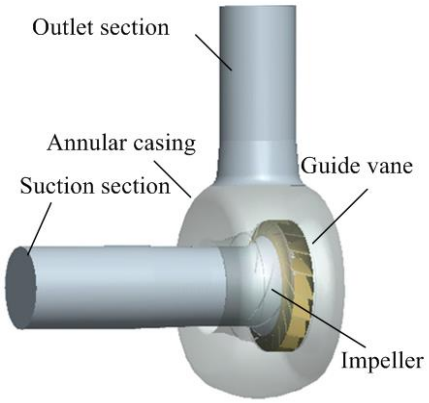

Figure 1. Sketch of flow-through components structure of model pump

In order to prevent the inlet and outlet velocity gradient from affecting the calculation results, the pump inlet and outlet are extended appropriately. Due to the complex structure of the nuclear main pump, we will adopt an adaptive unstructured tetrahedral mesh to divide the entire computational domain and continuously adjust the accuracy of the grid cells in order to observe poor quality grid areas in the grid, eliminate sharp vertexes in the fluid domain, reduce grid distortion rate and improve calculation accuracy. The computational domain was divided into a mesh using the pre-processing software Gambit. The most economical grid number of the model pump is a total of 5.9 million through grid-independent verification. The number elements for each flow-passing part is shown in Table 2. and the computational domain mesh is seen in figure 2.

Table 2. Detailed mesh information

Domain	impeller	guide vane	annular casing	Total
Number of elements($\times 10^3$)	1900	1520	1500	5900

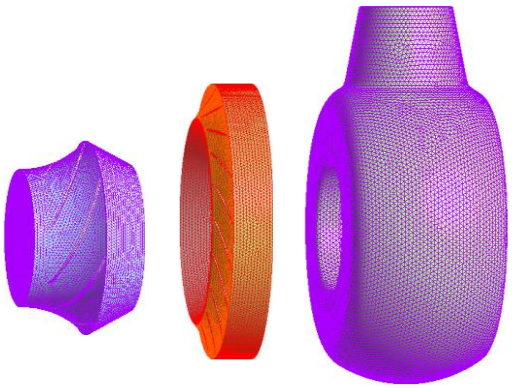

(a) Impeller (b) Guide vane (c) Annular casing

Figure 2. Meshing of computational domain

3. Numerical simulation and project design

3.1. Control equation and cavitation model

Cavitation flow can be seen as a homogeneous gas-liquid mixture. Each ingredient has the same speed and pressure and meets the non-slide conditions [10].The complicated flow field is analyzed using RANS equations in conjunction with governing equations as follows:

Continuity equation

$$\frac{\partial \rho}{\partial t}+\frac{\partial(\rho u_j)}{\partial x_j}=0 \quad (1)$$

Momentum equation

$$\frac{\partial(\rho u_j)}{\partial t}+\frac{\partial(\rho u_i u_j)}{\partial x_j}=\rho f_i-\frac{\partial \rho}{\partial x_i}+\frac{\partial}{\partial x_i}\left[(\mu+\mu_t)\left(\frac{\partial u_i}{\partial x_j}+\frac{\partial u_j}{\partial u_i}-\frac{2}{3}\frac{\partial u_k}{\partial x_k}\delta_{ij}\right)\right] \quad (2)$$

$$\rho=\rho_v\alpha_v+\rho_l(1-\alpha_l) \quad (3)$$

Where u is the flow velocity, ρ is the density, α is the volume fraction, μ &μ_t are the kinetic viscosity of mixed medium and the viscosity of turbulence, respectively. δ_{ij} is Kronecker delta and subscript *v*&*l* mean gas and liquid. The cavitation model uses the bubble growth equation based on Rayleigh-Plesset, namely:

$$R_B\frac{d^2R_B}{dt^2}+\frac{3}{2}\left(\frac{dR_B}{dt}\right)^2+\frac{2S}{R_B}=\frac{p_v-p}{\rho_f} \quad (4)$$

Where R_B is the radius of bubble and S means the coefficient of surface stretching force.

3.2. Numerical simulation method and boundary condition

ANSYS CFX software is used to simulate the full three-dimensional steady cavitation of the nuclear model pump in this paper. The Reynolds stress values were modeled using the RNG *k-ε* turbulence model because it has taken high anisotropy and vorticity of turbulence into account in the process and improve prediction accuracy for complex turbulence flows [11]. These features make it more reliable and accurate under the various flowing conditions. In general terms, the saturated vapor pressure of water at normal temperature (20 ℃) is 2338 Pa. The average diameter of the bubble is 2×10^{-6} m and the surface tension is 0.0717 N/m.The pressure and momentum equations are coupled by using the SIMPLEC algorithm with a high resolution scheme. The finite volume method is used to discretise the governing equations. The iterations are continued until the average residual error drops to 10^{-5}. The convergence of the numerical results is evaluated by monitoring the residual values and the pump outlet pressure [12]. The import boundary condition is Total Pressure. The export boundary condition is Mass Flow Rate. The non-slip boundary condition is used in the solid wall and the standard wall function is adopted in the near wall region. Cavitation inside the pump is achieved by gradually reducing the total pressure at the pump inlet. The mass flow outlet ensures that the pump can operate at the design conditions. Vapor phase volume fraction in the calculation of the initial flow is 0.

4. Results and Analysis

4.1. Experimental demonstration

In order to demonstrate the reliability of numerical calculation, the model test is carried out on a four quadrant test bench, as shown in figure 3. It consists of a suitable auxiliary pump, valves, pipelines and test instruments to form a test circuit. By turning on and off different auxiliary pumps and the corresponding valves, the direction of the liquid flow in the pipeline is changed, so that the normal and abnormal operating conditions of the pump are achieved. In the meantime, the numerical simulation results of the model pump are compared with the experimental results and the comparison results are shown in figure 4. As can be seen in figure 4, the calculated values of the model pump are in good agreement with the experimental results. Under the design conditions the simulated and actual head are 17.8m and 17.3m respectively and its error is not more than 2.8%. The simulated and actual efficiency are 84.4% and 82.5% respectively and its error is not more than 2.25%. Owing to deviating from the design conditions under the small and large flow rate conditions, there is a mismatch between the flow angle and the impeller as well as guide vane setting angles, which results in lower accuracy and an increase in head and efficiency calculation errors. However, the head error is less than 5.7% and the efficiency error does not exceed 7.2%.

Figure 3. Sketch of experimental setup

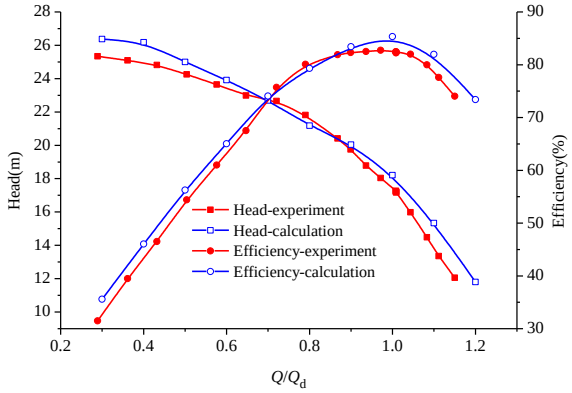

Figure 4. Characteristic curves of model pump

It can be shown in figure 5 that the main nuclear pump cavitation simulation and test results are basically identical and the changing trends are almost same. The simulated net positive suction head required (NPSHr) of the model pump is 4.87 m and the test value is 5.2 m, whose relative error is 4.1%.

In combining with the hydraulic performance test and cavitation test data as well as the error analysis of the model, the numerical calculation has certain accuracy and is validated for application within the research work.

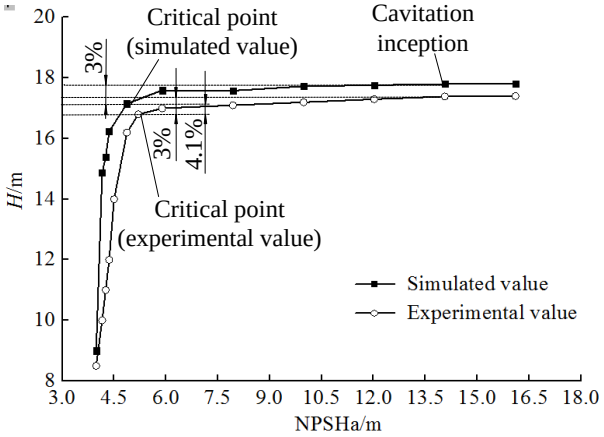

Figure 5. Results of cavitation simulation and experiment

4.2. Prediction of nuclear main pump cavitation characteristic curve

The cavitation performance of the pump is usually described by NPSHa-head relation. When the pump head reduces 3%, the NPSHa is the critical net positive suction head. In the pump cavitation external characteristic test, the NPSHa is defined as the difference between the pump inlet cross-section fluid energy and the saturated steam pressure [13]:

$$\mathrm{NPSHa} = \frac{p_{\mathrm{in}}}{\rho g} + \frac{v_{\mathrm{in}}^2}{2g} - \frac{p_{\mathrm{v}}}{\rho g} \qquad (5)$$

Where p_{in} is pump inlet pressure, v_{in} is the average velocity of pump inlet, p_{v} is saturated vapour pressure.

Under the premise of verifying the reliability of numerical calculation, the impeller cavitation can be divided into the following conditions, as shown in Fig.6. When NPSHa=16.11m, the pump works well; when NPSHa=9.98m, the pump head decreases 0.4% for cavitation inception; when NPSHa=5.89 m, the pump head decreases by 1.2% for the cavitation development; when NPSHa=4.87m, the pump head decreases by 3% for the critical cavitation state; when NPSHa=4.36m, the pump head decreases by 8.7%

for a serious stage of cavitation; when NPSHa=4.26m, the pump head decreases by 13.5% for the cavitation fracture state. Because the nuclear main pump in the actual operation process does not allow cavitation, this paper mainly focuses on the stage before the critical cavitation point.

4.3. Effect of cavitation flow on the performance of nuclear main pump

4.3.1. Effect of cavitation flow on the external characteristics of nuclear main pump

The pump inlet and outlet pressure and impeller torque can be attained by numerical simulation. The pump head, efficiency and power decline can be analyzed under the condition of cavitation respectively.

The head of pump:

$$H = \frac{p_{out} - p_{in}}{\rho g} \tag{6}$$

The capacity of pump:

$$P = M\omega \tag{7}$$

The efficiency of pump:

$$\eta = \frac{\rho g q_V H}{P} \tag{8}$$

Where ρ is medium density, g is acceleration of gravity, q_v is mass flow, M is the torque acting on the impeller blades, ω is angular velocity of rotation.

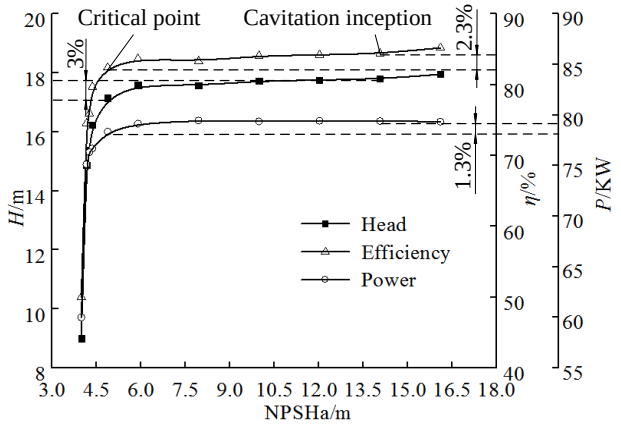

Figure 6. Curves of pump performance under different NPSHa value

As is shown in figure 6, with the degree of cavitation increasing, the changing trends of efficiency, pump head and capacity are basically the same. In the state of cavitation inception and development, pump head and efficiency declined slightly, but capacity almost unchanged. In the critical cavitation state, ie. NPSHa=4.87 m, the pump head, the efficiency and the capacity decrease by 3%, 2.3% and 1.3% respectively. In the serious cavitation condition, the pump head, efficiency and capacity show a steep downward trend. It can be seen that when cavitation happens in the nuclear main pump, the head, efficiency and capacity of the nuclear main pump are different in sensitivity to the reduction of the NPSHa. The head decreases the fastest and the capacity declines the slowest.

4.3.2. Effect of cavitation flow on the performance of flow-passing parts

The following formulas are applied to predict the hydraulic loss of both the guide vane and annular casing. The calculation method of the guide vane hydraulic loss is shown in formula (9):

$$\Delta H_{\text{guidevane}} = \frac{p_{\text{guidevaneoutlet}} - p_{\text{guidevaneinlet}}}{\rho g} \tag{9}$$

Where $\Delta H_{\text{guide vane}}$ is the hydraulic loss of guide vane, $p_{\text{guide vane outlet}}$ is the outlet total pressure of the impeller, $p_{\text{guide vane inlet}}$ is the inlet total pressure of guide vane.

The calculation method of annular casing hydraulic loss is shown in formula (10):

$$\Delta H_{\text{annularcasing}} = \frac{p_{\text{annularcasingoutlet}} - p_{\text{annularcasinginlet}}}{\rho g} \quad (10)$$

Where $\Delta H_{\text{annular casing}}$ is the hydraulic loss of the annular casing, $p_{\text{guide vane outlet}}$ is the outlet total pressure of the guide vane, $p_{\text{guide vane inlet}}$ is the inlet total pressure of guide vane.

Figure 7 shows the head and efficiency curves of impeller under different NPSHa values. It can be seen from Fig. 8 that when NPSHa=4.87m, the impeller head drops by 1% and the efficiency does not decrease. When NPSHa=4.36 m, the impeller head drops by 5.3% and the efficiency decreases by 2%. At this point, the impeller head and efficiency decline rapidly, the state of cavitation fracture occurs. It can be seen that the impact of cavitation on the head of impeller is also greater than the impact on efficiency.

It can also be seen from figure 6 and figure 7 that the changing trend of the head and efficiency with the decrease of NPSHa is basically same in the two cases of calculating the overall machine and the only impeller. Under the state of cavitation inception, the overall machine head is 17.8 m and the efficiency is 84.4%, while the impeller head is 19.9 m and the efficiency of impeller is 94.4%. The difference between them in head and efficiency are 10.5% and 10.6% respectively, mainly caused by the loss of flow due to the annular casing and guide vanes, the impact loss of the impeller entrance, the linear loss resulted from the inlet and outlet pipes and the numerical accuracy. The loss in guide vanes and casing is 1.84 m, accounting for 87.6% of the total loss. It can be seen that the loss of flow in guide vane and casing is the main reason for decreasing in head and efficiency.

When NPSHa=4.87 m, the pump head, the efficiency and impeller head decrease by3%, 2.3% and 1% respectively, but the efficiency does not decline. These differences of decline are mainly caused by the loss of casing and guide vane.

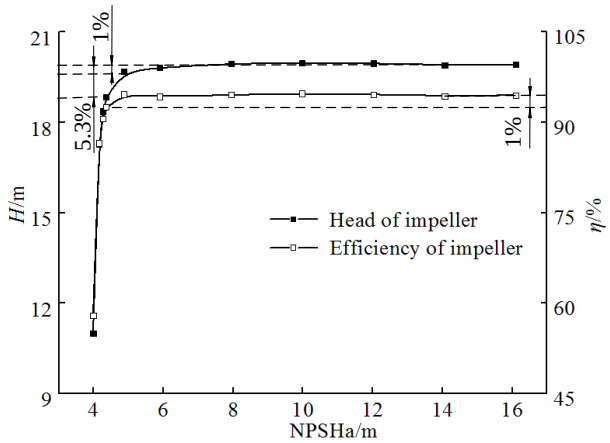

Figure 7. Head and efficiency curves of impeller under different NPSHa values

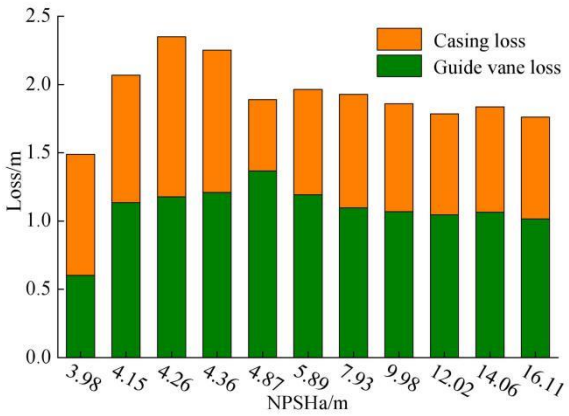

Figure 8. The loss histogram of guide vane and annular casing under different NPSHa value

Figure 8 is the loss histogram of guide vane and annular casing under different NPSHa value. As can be seen in figure 8, the loss in guide vane increases firstly and then decreases with the degree of cavitation increasing. The loss of guide vane is unchanged in the cavitation inception and development state. The loss in guide vanes increases and reaches a maximum value in the critical cavitation condition and then the loss gradually decreases. The loss of casing in the cavitation inception and development state changes lightly. It has a minimum value in the critical cavitation state and shows the trend of increasing first and then decreasing after the critical cavitation state. With the degree of cavitation aggravating, the overall loss of casing and guide vane increases first and then decreases. In the cavitation fracture state, namely NPSHa=4.26 m, there is a maximum value. While in the critical cavitation state, namely NPSHa=4.87 m, there is a minimum value. The loss change of guide vane and

casing mainly caused by cavitation which interferences downstream flow field in the impeller. Owing to the overall loss of guide vane and casing changes little before the critical cavitation, this paper mainly analyzes the distribution law of the internal flow field in the impeller rather than casing and guide vane.

4.4. Internal cavitation development law of nuclear main pump impeller

Figure 9 shows the distribution of bubble volume fraction under different cavitations in the steady cavitation calculation. The bubble surface is defined as the equivalent surface of 10% bubble volume rate. When the inlet pressure of the nuclear main pump gradually decreases, the pressure inside the impeller will also decrease. When the partial pressure inside the impeller is lower than the saturated vapor pressure of the liquid, cavitation will occur and bubbles will be generated. At this time, the bubbles are mainly concentrated on the suction side of the blade near the front cover board. As shown in figure 9 (a), the area of cavitation in the impeller is small and the flow passage has a little effect on the flowing. This is called cavitation inception. The pump performance is almost unchanged in this state.

With the further reduction of the NPSHa, the cavitation in the impeller continues to develop.The cavitation area of the blade suction surface increases and the air bubbles gradually extend to the outlet and the back-end plate of the impeller along the surface of the blade. Finally the bubbles accumulate near the one side of the suction surface. As shown in figure 9 (b) and (c), this is the state of cavitation development.

With the development of cavitation, the bubbles on the front cover board of the suction side have spread to the middle of the blade. The bubble area on the back-end plate also gradually increases and the accumulated degree of bubbles on the suction side of the blade increases. As shown in figure 9 (d), the development of the impeller cavitation has an impact on energy exchange, which makes the pump performance decline. At this point, it is the critical cavitation state.

With the degree of cavitation aggravating, the bubbles on the suction surface of the blade continues to extend toward the outlet of the impeller, while the bubbles on the suction surface accumulates further and blocks the flow passage, which greatly reduces the pump performance. As shown in figure 9 (e), it is the serious cavitation condition.

When the degree of cavitation is further aggravated, a large number of bubbles accumulate in the impeller passage, causing serious blockage, limiting the flow area, affecting normal fluid flow and causing the state of cavitation fracture, as shown in figure 9 (f). These above processes correspond to the curves of NPSHa-*H* relation in figure 4. It can also be seen from figure 9, the distribution of bubbles on the blade is uneven and with the degree of cavitation increasing, the unevenness of the air bubbles in the impeller gradually reduces.

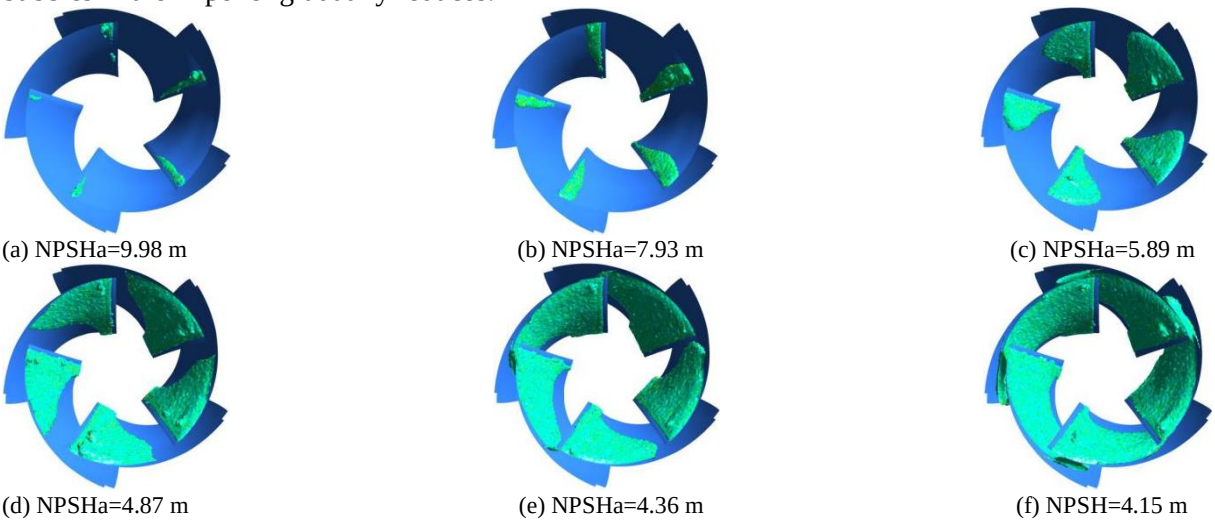

(a) NPSHa=9.98 m (b) NPSHa=7.93 m (c) NPSHa=5.89 m

(d) NPSHa=4.87 m (e) NPSHa=4.36 m (f) NPSH=4.15 m

Figure 9. Development of cavitation in nuclear main pump

4.5. Internal flow-field characteristics of nuclear main pump impeller under cavitation condition

Figure 10 shows the variation of turbulence dissipation rate along the flow passage on the water-carrying section of the impeller under the different cavitations. The abscissa 'denotes' means the relative length of the midline from the inlet to the outlet of impeller, denoted by S, where 0 & 1 represent the inlet and outlet of impeller respectively. The ordinate means the average value of the turbulence dissipation rate at different radius of the impeller. Turbulent dissipation rate refers to the rate at which turbulent kinetic energy is converted into kinetic energy of molecular heat movement by molecular viscosity effect. It can be seen from figure 10 that the overall trend of turbulent dissipation rate along the flow passage of impeller is hump shape. As the degree of cavitation aggravates, the turbulence dissipation rate in impeller varies greatly. The rate of change in turbulent dissipation at the relative position of S=0~0.3 in the impeller flow passage and the outlet of the impeller is very little with the cavitation aggravating. In the vicinity of the relative position of S=0.3~1.0, the turbulence dissipation rate gradually decreases with the cavitation degree aggravating and this region moves to the impeller outlet. This is because the bubble area increases and the outlet of impeller extends due to the cavitation development. The dynamic viscosity of bubbles is much smaller than that of water, resulting in the decrease of the turbulence dissipation rate.

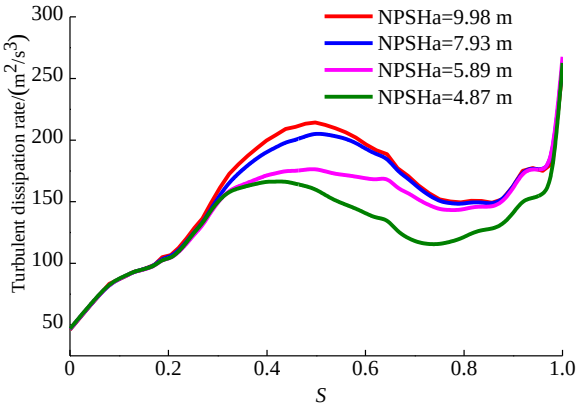

Figure10. Turbulent dissipation curves in the impeller passage

5. Conclusion

1)The results show that the head, efficiency and power of the nuclear main pump have different sensitivities to the reduction of NPSHa. With the development of the cavitation, the head declines most sharply and the power most moderately.

2) Under the cavitation condition, bubbles generated by cavitation have a squeezing effect on the impeller flow passage. The area of the carrying-water section reduces and the relative velocity of the fluid increases.

3) When cavitation occurs in the nuclear main pump, the generation of bubbles changes the state of the fluid in the cavitation zone, reducing the fluid dynamic viscosity and resulting in the decrease of the turbulence dissipation rate and the turbulence dissipation loss.

Acknowledgements

The authors are grateful to the financial support from the National Natural Science Foundation of China (Research Project No.51469013).

References

[1] G.J. Zhou, Z.Y. Yan and S.X. Xu 2000 *Fluid Mechanics* (Beijing: Higher Education Press)
[2] Brennen C E 2013 *Cavitation and bubble dynamics* (Cambridge: Cambridge University Press)
[3] Knapp R T, Daily J W and Hammitt F G 1970 *Cavitation* (New York: McGraw-Hill)

[4] X.R. Cheng, W.R. Bao,L. Fu and X.T. Ye. Sensitivity analysis of nuclear main pump annular casing tongue blend. *Advances in Mechanical Engineering*, 2017, **9**(7) 1-9.
[5] J.X. Lu,S.Q. Yuan, Siva P,J.P. Yuan,X.D. Ren and B.L. Zhou. The characteristics investigation under the unsteady cavitation condition in a centrifugal pump. *Journal of Mechanical Science & Technology*, 2017, **31**(3) 1213-1222.
[6] L.P. Chai, H. Ye,Z.M. Ren and H. Li. Analysis of impeller geometric parameters affecting the centrifugal pump cavitation performance based on CFD simulations. *Journal of Drainage and Irrigation Machinery Engineering*, 2016, **34**(8) 645-650.
[7] F.M. Zhou and X.F. Wang. Effects of staggered blades on the hydraulic characteristics of a 1400-MW canned nuclear coolant pump. *Advances in Mechanical Engineering*,2016, **8**(8) 1-21.
[8] Y.Q. Li, S.W. Yuan and H.X. Lai. Numerical Study of Unsteady Flows with Cavitation in a High-Speed Micro Centrifugal Pump. *Journal of Thermal Science*, 2017, **26**(1) 18-24.
[9] X.M. Guo, Z.C. Zhu, B.L. Cui and Y. Li. Effects of the short blade locations on the anti-cavitation performance of the splitter-bladed inducer and the pump. *Chinese Journal of Chemical Engineering*, 2015, **23**(7) 1095-1101.
[10] Q.R. Si, S.Q. Yuan, X.J. Li, J.P. Yuan and J.X. Lu. Numerical simulation of unsteady cavitation flow in the casing of a centrifugal pump. *Transactions of the Chinese Society of Agricultural Machinery*, 2014, **45**(5) 84-90.
[11] H. Bing, S.L. Cao and Y.C. Wang. Influence of turbulence model on performance prediction of Mixed-flow Pump. *Transactions of the Chinese Society for Agricultural Machinery*, 2013, **44**(11) 42-47.
[12] X.Y. Wang, C.X. Wang and Y.B. Li. Numerical study of flow characteristics in the impeller side chamber of centrifugal pump. *Transactions of the Chinese Society for Agricultural Machinery*,2009, **40**(4) 75-80.
[13] S.L. Wang, L.Tan and Y.C. Wang. Characteristics of transient cavitation flow and pressure fluctuation for a centrifugal pump. *Journal of Vibration and Shock*, 2013, **32**(22) 168-173.